

# 郟庐断裂带(安徽段)内磁铁石榴角闪岩的形成条件、年代学及构造归属的探究<sup>\*</sup>

聂峰 石永红<sup>\*\*</sup> 王娟 康涛 曹晟

NIE Feng, SHI YongHong<sup>\*\*</sup>, WANG Juan, KANG Tao and CAO Sheng

合肥工业大学资源与环境工程学院, 合肥 230009

School of Resources and Environment Engineering, Hefei University of Technology, Hefei 230009, China

2014-03-05 收稿, 2014-04-01 改回.

Nie F, Shi YH, Wang J, Kang T and Cao S. 2014. Investigation on the metamorphic conditions and geochronology for the magnet garnet amphibole in the Tan-Lu Fault Zone (Anhui segment), and discussion of its tectonic attribution. *Acta Petrologica Sinica*, 30(6):1718–1730

**Abstract** Based on the research of tectonic geology and lithology, The magnet garnet amphibole and its adjacent rock occurs as the tectonic lens in the south of Feidong terrane. This metamorphic rocks contain two metamorphic assemblages from different stages, and the  $P$ - $T$  estimates show that the  $P$ - $T$  condition of ① stage is  $T=616\sim 700^{\circ}\text{C}$  and  $P=0.66\sim 0.85\text{GPa}$  respectively and the average  $T$  and  $P$  are  $653\pm 35^{\circ}\text{C}$  and  $0.75\pm 0.09\text{GPa}$ ; Differentially, the ② stage is  $T=616\sim 700^{\circ}\text{C}$  and  $P=0.66\sim 0.85\text{GPa}$ , and average  $P$ - $T$  condition is  $653\pm 35^{\circ}\text{C}$  and  $0.75\pm 0.09\text{GPa}$ . A rapid and slight Isobaric cooling process is indicated by features from the first stage to the second stage. According to the Raman Spectral Analysis and the LA-ICPMS dating, the metamorphic age of the magnet garnet amphibole is  $2469\pm 49\text{Ma}$ . Combined with geological background and current situation, The magnet garnet amphibole maybe come from north china plate because of the sinistral strike-slip of Tan-Lu Fault Zone, It could be further theorized that the width of Tan-Lu Fault Zone is up to 10~15km.

**Key words** Magnet garnet amphibole; Isobaric cooling; Zircon U-Pb age; Tan-Lu Fault Zone

**摘要** 通过对肥东群南缘特征性岩石——磁铁石榴角闪岩的构造地质学和岩相学研究表明,磁铁石榴角闪岩及其围岩以构造透镜体形式产出,该变质岩具有两个阶段变质矿物组合,热力学评价显示①阶段的温压范围为: $T=616\sim 700^{\circ}\text{C}$ 和 $P=0.66\sim 0.85\text{GPa}$ ,平均温压为 $\bar{T}=653\pm 35^{\circ}\text{C}$ 和 $\bar{P}=0.75\pm 0.09\text{GPa}$ 。②阶段的温压范围为: $T=597\sim 643^{\circ}\text{C}$ 和 $P=0.51\sim 0.94\text{GPa}$ ,平均温压为 $\bar{T}=620\pm 15^{\circ}\text{C}$ 和 $\bar{P}=0.73\pm 0.15\text{GPa}$ ,并表现出一个快速等压降温 $P$ - $T$ 演化特征。锆石 U-Pb 定年和拉曼光谱分析表明,该磁铁石榴角闪岩的变质年龄为 $2469\pm 49\text{Ma}$ 。结合地质背景和前人的研究,可以判定该类岩石可能源于华北板块。由于郟庐断裂的左旋走滑作用被构造并置与扬子板块中。从而进一步推测,郟庐断裂(安徽段)横向宽度可达到10~15km。

**关键词** 磁铁石榴角闪岩;等压降温;锆石 U-Pb 年龄;郟庐断裂

**中图法分类号** P588.345; P597.3

## 1 引言

长期以来,郟庐断裂的形成机制和演化过程一直是研究的热点,特别是该断裂与大别-苏鲁造山带在时空上、成因上

的联系一直为人们所关注(Xu *et al.*, 1987; Zhu *et al.*, 2005, 2009, 2010)。目前,主流的观点认为郟庐断裂形成于大别-苏鲁造山带碰撞俯冲过程中(Zhang *et al.*, 1984; Hsu *et al.*, 1987; Watson *et al.*, 1987; Yin and Nie, 1993; Li,

<sup>\*</sup> 本文受国家自然科学基金项目(41272073)和国家科技重大专项(2011ZX05008-001-31)联合资助。

第一作者简介:聂峰,男,1989年生,硕士生,地质工程专业,E-mail: HFUT\_niefeng@163.com

<sup>\*\*</sup> 通讯作者:石永红,男,1968年生,博士,教授,变质地质学专业,E-mail: yonghongshi3110@sohu.com

1994; 万天丰和朱鸿, 1996; Chang, 1996; 王小凤等, 1998; Chung, 1999; Zhu *et al.*, 2005, 2009, 2010)。另一种观点则强调郟庐断裂形成于该造山带折返之后(Xu *et al.*, 1987; Okay and Sengor, 1992; Xu and Zhu, 1994; Wang *et al.*, 2003; Meng *et al.*, 2007)。近年来对郟庐断裂的研究多集中于年代学和构造地质学方面(Xu *et al.*, 1980, 1987, 1994; Lin and Fuller, 1990; Okay and Sengor, 1992; Yin and Nie,

1993; Li, 1994; Lin *et al.*, 2005, 2009; Lin and Li, 1995; Zhang, 1997; Gilder *et al.*, 1999; Schmid *et al.*, 1999; Wang *et al.*, 2003; Meng *et al.*, 2007; Zhu *et al.*, 2005, 2009, 2010; 朱光等, 1998, 2001, 2002, 2003, 2005a, b, 2006a, b, 2009a; 王勇生等, 2004, 2005a, b, 2006; 牛漫兰等, 2002, 2005, 2006; Zhang and Teyssier, 2013; Zhang *et al.*, 2013; 赵田等, 2014), 多关注其不同层次的变形特征和水平

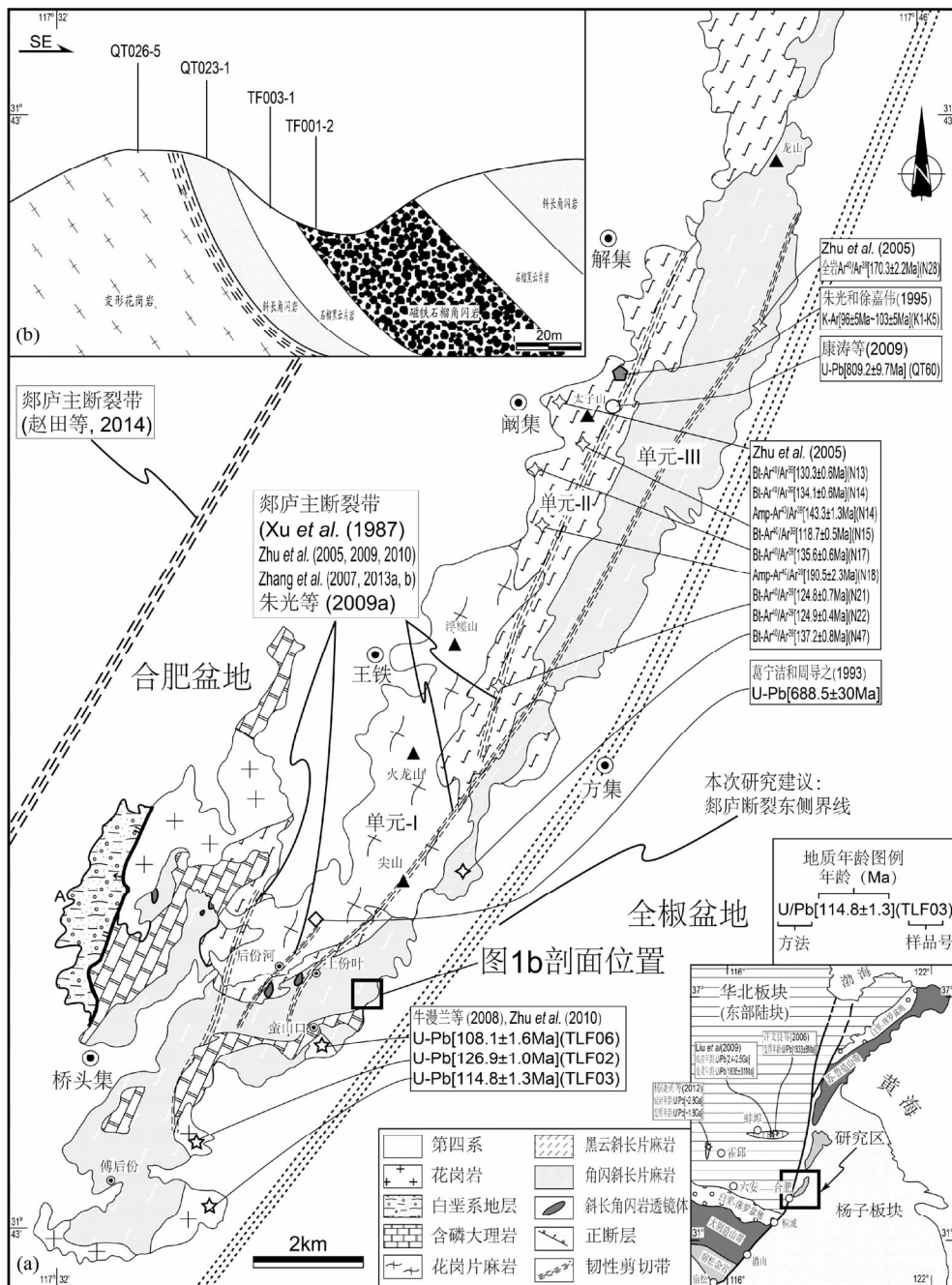


图1 研究区地质简图

(a)-肥东地区(安徽段)地质图;(b)-地质剖面图

Fig.1 Simplified geological sketch map of the study area

(a)-geological sketch map of the Feidong area (Anhui segment); (b)-geological profile

错断距离 (Zhu *et al.*, 2005, 2009, 2010)。而对于郟庐主干断裂(安徽段)空间上的展布状况仍缺乏统一的认识。Xu *et al.* (1987)、Zhang *et al.* (2007, 2013a, b)、Zhu *et al.* (2005, 2009, 2010) 认为郟庐主干断裂位于合肥盆地东缘,即解集-阚集-王铁-桥头集以东的张八岭隆起区。但是,赵田等(2014)则认为该主干断裂处于合肥盆地内部(图1)。关于该断裂带的横向展布,多数学者认为其沿着一个狭窄的线性条带分布,并仅限于扬子地块上。上述关于郟庐断裂带空间位置的不同认识,可能是由于对张八岭隆起区岩石单元构成缺乏深入的解剖所致,特别是相关精细的变质岩石学研究的不足,影响了人们对郟庐断裂带的全面深入理解。作为切穿了华北和扬子两大板块的郟庐断裂带,其展布范围可能不仅局限于扬子板块上,横向上的范围应当较为宽阔,从而部分进入华北板块内。若如此,在走滑断裂作用下,该带内可能有来自两侧板块的岩石。为此,本文对张八岭隆起区肥东群的特征性岩石——磁铁石榴角闪岩进行了详细变质岩石学、年代学研究。研究显示,该类岩石可能来源于华北板块,推测其可能因郟庐断裂的走滑作用被卷入该带内。

## 2 研究剖面及样品介绍

本次研究区域位于张八岭隆起区南段肥东地块最南缘。该地块西侧为合肥盆地,东侧为全椒盆地所覆盖(图1)。根据Zhu *et al.* (2005, 2009, 2010)和康涛等(2013)的研究,认为该地块自西向东可分为3个单元:(1)单元-I:主体为花岗岩片麻岩,沿浮渣山-火龙山-尖山-后分河一线分布,其间夹有斜长角闪岩和黑云斜长片麻岩透镜体;(2)单元-II:主要为黑云斜长片麻岩,分布于太子山一线;(3)单元-III:主要由角闪斜长片麻岩、含磷大理岩、斜长角闪岩、石榴黑云母片麻岩构成,沿龙山-方集-上份叶-蛮山口分布。该地块中发育有3条NNE向韧性剪切带,每条宽度在100~200m(图1a),均表现为左旋走滑运动特征(Zhu *et al.*, 2005, 2009, 2010)。

重点研究的剖面位于单元-III东南缘,蛮山口北东,上份叶东南,坐标为:纬度31°46.148'和经度117°36.663',剖面总长约200m。在该剖面上共采集23块样品,其中变形花岗岩5块,斜长角闪岩3块,石榴黑云片岩7块,磁铁石榴角闪岩8块,其中用于此次研究分析的共计4块(图1b),分别为QT026-1、QT023-1、TF003-1和TF001-2。研究剖面为NW-SE向,由西向东出露的岩性依次为变形花岗岩、斜长角闪岩、石榴黑云片岩、磁铁石榴角闪岩、石榴黑云片岩和斜长角闪岩(图1b、图2a)。这些岩石均以单斜层形式产出,面理倾向为134°~166°、倾角47°~65°。其中磁铁石榴角闪岩夹持于石榴黑云片岩之中,其出露的宽度约40~60m,斜长角闪岩和石榴黑云片岩宽度多在20~30m(图2a),这三类岩石紧密共生,沿走向延伸<300m,表现为构造透镜体形式。而变形花岗岩则沿走向稳定延伸,并与斜长角闪岩顺层接触,露头规模可见到微褶和长石拉长变形之特征(图2a)。

表1 磁铁石榴角闪岩代表性矿物成分(wt%)

Table 1 The representative mineral compositions (wt%) of magnet garnet amphibole

矿物	包体			基质1			基质2		
	Grt	Gru	Fe-Hbl	Grt	Gru	Fe-Hbl	Grt	Gru	Fe-Hbl
SiO <sub>2</sub>	36.47	47.94	42.64	36.48	50.48	41.28	36.17	50.32	40.76
TiO <sub>2</sub>	0.00	0.00	0.00	0.00	0.02	0.03	0.00	0.00	0.13
Al <sub>2</sub> O <sub>3</sub>	19.92	0.44	10.93	20.25	1.12	12.80	20.01	0.96	13.60
FeO	33.02	37.89	27.17	33.68	39.08	28.18	33.81	39.47	28.14
Cr <sub>2</sub> O <sub>3</sub>	0.00	0.00	0.00	0.01	0.00	0.00	0.03	0.00	0.00
MnO	1.18	0.16	0.05	1.14	0.14	0.05	1.08	0.15	0.05
MgO	0.77	6.57	3.76	0.68	5.41	2.64	0.89	5.47	2.36
CaO	8.09	0.62	11.45	7.25	1.27	11.51	7.04	0.99	11.78
Na <sub>2</sub> O	0.03	0.31	1.44	0.03	0.27	1.56	0.04	0.21	1.64
K <sub>2</sub> O	0.00	0.01	0.09	0.00	0.01	0.11	0.00	0.01	0.10
Total	99.47	93.94	97.54	99.53	97.79	98.16	99.06	97.57	98.55
O	12.00	23.00	23.00	12.00	23.00	23.00	12.00	23.00	23.00
Si	2.96	7.92	6.61	2.97	7.98	6.39	2.96	7.99	6.31
Al	1.91	0.09	2.00	1.94	0.21	2.34	1.93	0.18	2.48
Fe <sup>3+</sup>	0.16	0.00	0.54	0.12	0.00	0.56	0.16	0.00	0.45
Ti	0.00	0.00	0.00	0.00	0.00	0.00	0.00	0.00	0.02
Cr	0.00	0.00	0.00	0.00	0.00	0.00	0.00	0.00	0.00
Fe <sup>2+</sup>	2.08	5.23	2.99	2.17	5.17	3.09	2.15	5.24	3.20
Mn	0.08	0.02	0.01	0.08	0.02	0.01	0.08	0.02	0.01
Mg	0.09	1.62	0.87	0.08	1.28	0.61	0.11	1.30	0.54
Ca	0.71	0.11	1.90	0.63	0.22	1.91	0.62	0.17	1.96
Na	0.01	0.10	0.43	0.00	0.08	0.47	0.01	0.06	0.49
K	0.00	0.00	0.02	0.00	0.00	0.02	0.00	0.00	0.02
Sum	8.00	15.09	15.35	8.00	14.95	15.40	8.00	14.95	15.47

## 3 岩相学和主要矿物化学分析

由于此次研究的重点是磁铁石榴角闪岩,故矿物化学分析主要是针对该类岩石进行。矿物成分测试由合肥工业大学资源与环境工程学院电子探针实验室完成,仪器型号为JEOL JAX-8230,实验条件为:加速电压15kV,电子束流20nA,电子束斑为3 $\mu$ m。其中石榴石和铁闪石、铁普通角闪石结构式分别以12和23个O进行计算,Fe<sup>2+</sup>的校正则分别以电价平衡法(Droop, 1987)、全Fe<sup>2+</sup>和Si+Al+Ti+Mg+Fe+Mn=13进行估算。代表性矿物分析结果见表1。此外,文中矿物缩写据Whitney and Evans (2010):Grt=石榴石;Gru=铁闪石;Fe-Hbl=铁普通角闪石;Fe-Ts=铁契尔马克闪石;Qz=石英;Amp=角闪石;PL=斜长石;Kfs=钾长石;Bt=黑云母;Ms=白云母;Mag=磁铁矿;Chl=绿泥石;Ap=磷灰石。

### 3.1 岩相学分析

(1)变形花岗岩(样品QT026-5):主要为钾长石(20%~25%)+斜长石(20%)+石英(30%)+黑云母(10%)+白云母(10%~15%)(图2b)。这些矿物因剪切变形作用,多表现为拉长变形之特征,粒径大小不一。其中钾长石粒径为0.2~0.5mm,斜长石粒径为0.2~0.5mm,石英粒径为0.2~0.5mm;黑云母则表现为他形-半自形,粒径约0.2~0.3mm。

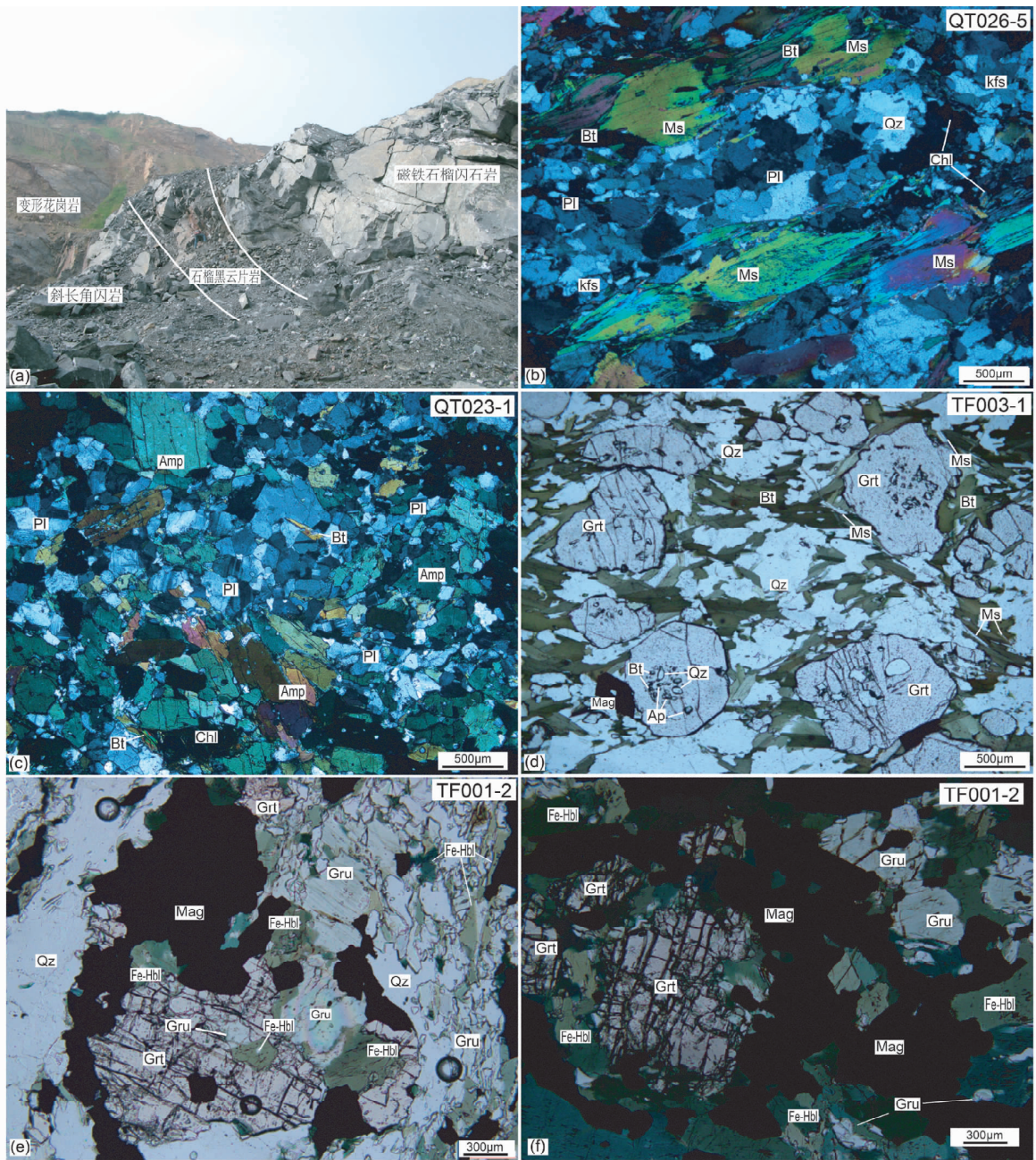


图2 研究区岩石野外照片和显微照片

(a)-主要岩性接触关系；(b)-变形花岗岩显微照片；(c)-斜长角闪岩显微照片；(d)-石榴黑云片岩显微照片；(e、f)-磁铁石榴角闪岩显微照片

Fig.2 The field photos and microstructure photos in the study area

(a)-contact relation of main lithology；(b)-microstructure photos of deformational granites；(c)-microstructure photos of Plagioclase amphibolite；(d)-microstructure photos of garnet biotite schist；(e, f)-microstructure photos of magnet garnet amphibole

白云母则多为多硅白云母,  $Si^{4+}$  多在 3.08 ~ 3.12。

(2) 斜长角闪岩 (样品 QT023-1): 组成矿物为角闪石 (50% ~ 55%) + 斜长石 (20% ~ 25%) + 石英 (10% ~ 15%) + 黑云母 (10% ~ 15%) + 磷灰石 (5%) (图 2c)。角闪石呈自形-半自形, 鳞片状定向排列, 粒径 0.2 ~ 2mm, 颗粒边缘发生轻微绿泥石化; 斜长石为半自形-他形结构, 粒径为 0.1 ~

0.3mm; 黑云母半自形-他形, 粒径大小 ~ 0.2mm, 部分颗粒已完全退变为绿泥石, 仅保留黑云母结构假象; 石英他形结构, 粒径大小 0.2 ~ 0.5mm; 磷灰石他形结构, 颗粒大小为 0.1 ~ 0.3mm。

(3) 石榴黑云母片岩 (样品 TF003-1): 矿物组成为石榴石 (30%) + 黑云母 (40%) + 石英 (20%) + 白云母 (10%) +

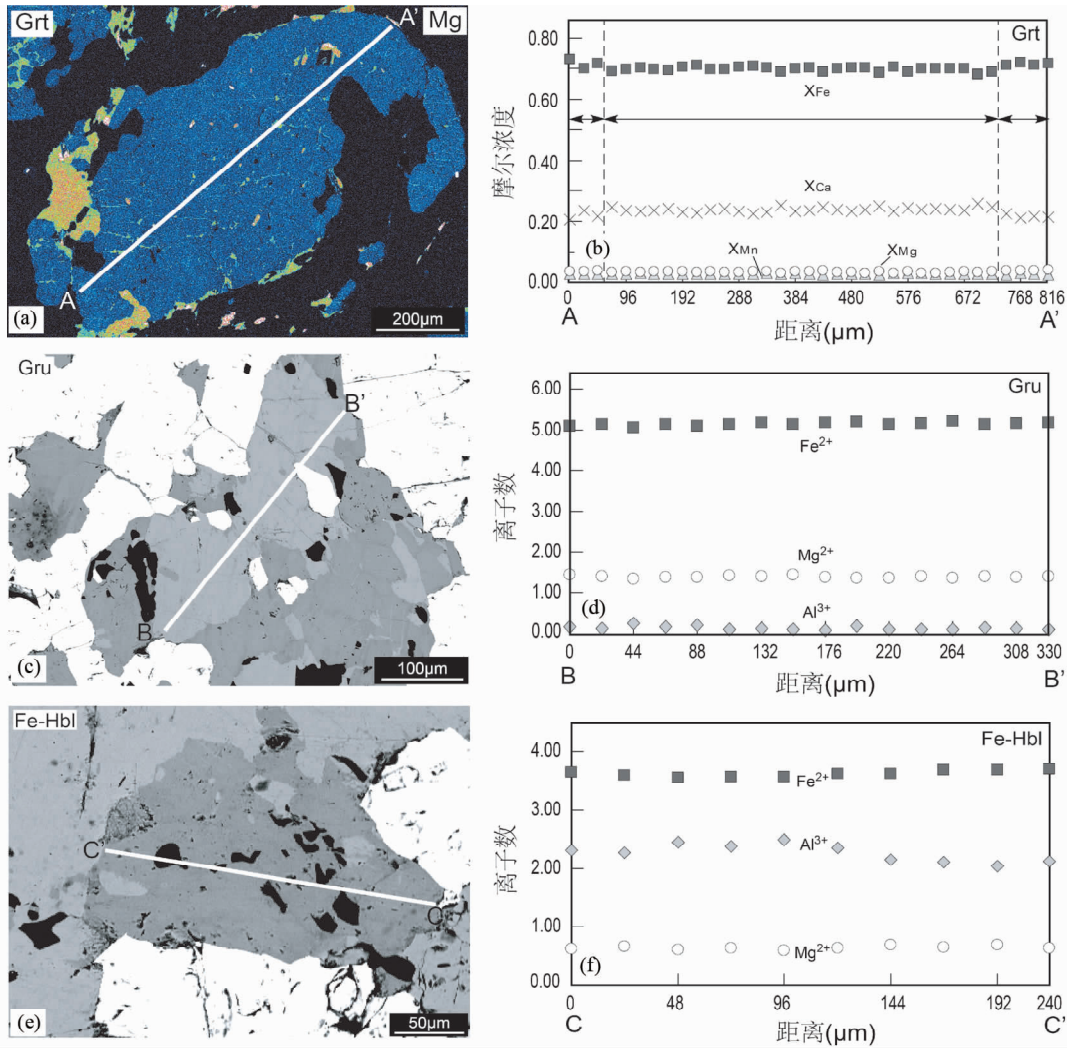


图3 磁铁石榴角闪岩的石榴石 X-ray mapping 图、角闪石 BSE 图及成分剖面图

(a)-石榴石 X-ray mapping 图; (b)-石榴石成分剖面图; (c)-铁闪石 BSE 图; (d)-铁闪石成分剖面图; (e)-铁普通角闪石 BSE 图; (f)-铁普通角闪石成分剖面图

Fig. 3 X-ray mapping image of garnet, BSE images of amphibole and compositional profiles from magnet garnet amphibole

(a)-X-ray mapping image of garnet; (b)-compositional profiles of garnet; (c)-BSE image of grunerite; (d)-compositional profiles of grunerite; (e)-BSE image of Fe-hornblende; (f)-compositional profiles of Fe-hornblende

磁铁矿(5%) + 磷灰石(3%)(图 2d), 石榴石呈自形-半自形, 粒径 1 ~ 3mm, 内含大量石英、云母、磷灰石包体, 包体主要分布于核部, 边部无包体; 黑云母为自形-半自形结构, 粒径大小 0.2 ~ 1mm。白云母为自形-半自形, 粒径 0.2 ~ 0.5mm, 夹持于黑云母之间; 石英呈他形, 粒径 0.2 ~ 3mm; 磁铁矿呈自形, 粒径 0.2 ~ 0.3mm。

(4) 磁铁石榴角闪岩(样品 TF001-2): 该类岩石是本次分析的重点岩石, 其矿物组合为石榴石(10% ~ 15%) + 铁普通角闪石(20% ~ 25%) + 铁闪石(25% ~ 30%) + 磁铁矿(25% ~ 30%) + 石英(10% ~ 15%) + 磷灰石(1% ~ 3%)(图 2e, f)。石榴石呈半自形-他形, 粒径约为 0.5 ~ 5mm, 内部包含铁闪石、铁普通角闪石、磁铁矿、石英包体(图 2e, f), 其多破裂, 裂隙之中常常被绿泥石所充填; 铁闪石以基质和

包体两种形式存在, 其中基质中的的铁闪石呈他形, 粒径 0.1 ~ 0.5mm; 铁普通角闪同样以包体和基质两种形式存在, 基质中的铁普通角闪石为他形, 粒径 0.1 ~ 1mm, 其边缘或裂隙常常被绿泥石所替代; 石英为他形, 粒径 0.1 ~ 2mm; 磁铁矿呈自形-他形, 粒径 0.1 ~ 3mm; 磷灰石为他形, 粒径 0.1 ~ 0.2mm。

### 3.2 磁铁石榴角闪岩主要矿物化学分析

为了较为精确地揭示该类岩石中主要矿物成分变化特征, 以及准确评价其 *P-T* 演化过程, 本次研究对其中的石榴石、角闪石进行了细致的成分剖面研究。研究显示:

(1) 石榴石: 在 X-ray Mapping 图中(图 3a), 其无明显的

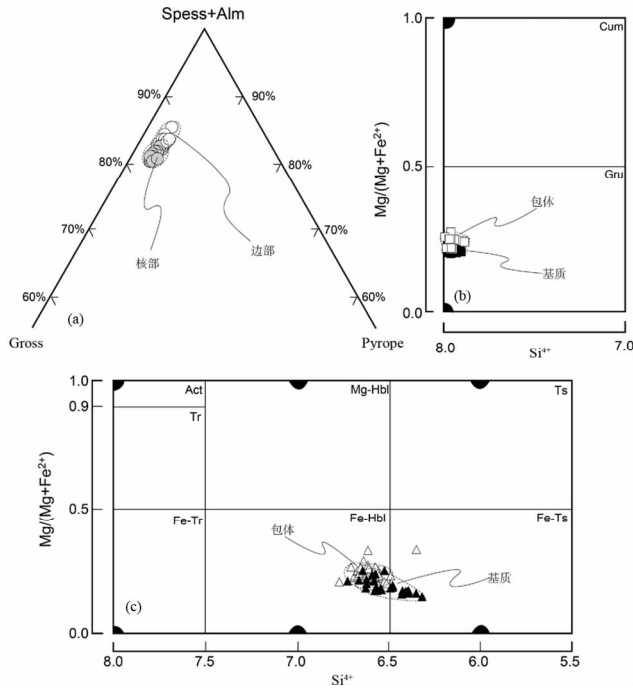


图4 矿物成分图  
 (a)-石榴石成分三角图; (b)-铁闪石成分图; (c)-铁普通角闪石成分图  
 Fig. 4 Compositional diagrams of the metamorphic minerals  
 (a)-compositional triangle of garnet; (b)-compositional diagrams of grunerite; (c)-compositional diagrams of Fe-hornblende

环带特征,颜色较为均匀。但在成分剖面中(图3b),石榴石显示了轻微的核、边结构。自核部至边部,铁铝榴石组分逐渐增高(64%核→73%边),镁铝榴石组分轻微增高(3%核→5%边),钙铝榴石组分则略微降低(15%核→11%边),锰铝榴石组分较为平坦。同样地,在成分三角图中(图4a),核、边成分也略显差异,其中铁铝榴石组分逐渐增高,镁铝榴石组分和钙铝榴石组分相对较低。但就总体而言,石榴石成分变化似乎并不显著,这意味着其可能处于快速生长条件下,并已达到均一化程度。

(2)角闪石:该类岩石具有铁闪石和铁普通角闪石两种闪石,且两者都以包体和基质形式存在(图2e)。对基质中的铁闪石和铁普通角闪石的定量分析显示,无论是在矿物颜色方面,还是矿物成分方面,这两个闪石均较为均匀,没有明显的环带特征(图3c-f)。其中铁闪石中的 $Fe^{2+}$ 、 $Mg^{2+}$ 和 $Al^{3+}$ 成分十分平坦,没有早期或后期变质作用的叠加。稍有不同的是铁普通角闪石 $Al^{3+}$ 自核部至边部轻微降低(2.5核部→2.0边部)。参照Hammarstrom *et al.* (1986)、Hollister *et al.* (1987)、Johnson *et al.* (1989)和Schmidt. (1992)的研究,我们推测这也许反映的是一种降压的过程。然而,从成分剖面看(图3f),这种退变降压可能并不显著。此外,以基质和包体形式存在的两种闪石的成分也没有显著的成分差异(图4b, c)。其中基质和包体的铁闪石成分变化基本位于同一

个区域(图4b),略有差异的是包体中的 $Mg/(Fe^{2+} + Mg)$ 比值略高于基质的 $Mg/(Fe^{2+} + Mg)$ 。对于包体中的铁普通角闪石其严格位于Fe-Hbl区域,而基质中铁普通角闪石主体位于Fe-Hbl区域,部分落入Fe-Ts区域(图4c)。

#### 4 磁铁石榴角闪岩峰期变质 P-T 条件评价

依据岩相学和矿物化学分析(图2e, f、图3),大致可以判定磁铁石榴角闪岩可能具有两个阶段的变质矿物组合:①阶段:Grt-I(核部)+Gru(包体)+Fe-Hbl(包体)+Qtz(包体)+Mag(包体);②阶段:Grt-II(边部)+Gru(基质)+Fe-Hbl(基质)+Qtz(基质)+Mag(基质)+Ap磷灰石(基质)。据此,本文对其进行了细致的温压评价。在成分选取方面,参照成分剖面的分析(图2e, f、图3),①阶段变质的成分选取石榴石核部,以及石榴石包体中的铁闪石、铁普通角闪石进行计算;②阶段变质的成分选取石榴石边部,基质中的铁闪石、铁普通角闪石核部或近边部的成分进行计算。同时,为保证分析计算的统计意义,本次研究在基质中共选取12个矿物对,包体中选取6个矿物对进行温压估算。基于Worley and Powell (2000)、Powell and Holland (2008)和魏春景等(2009)的研究,此次P-T条件的评价选用了Thermocalc version 3.33 (Holland and Powell, 1998)平均温压法(av-PT)进行,计算结果见表2。由于①和②阶段的矿物组合基本类似,因此,这两个阶段的PT值基本是由6条独立反应线限定:

表2 磁铁石榴角闪岩 P(GPa)-T(°C) 条件

Table 2 The P-T conditions for magnet garnet amphibole

样品	T	P	$\sigma T$	$\sigma P$	$\sigma fit$
包体					
1	700	0.66	249	0.67	3.22
2	688	0.67	215	0.59	2.66
3	652	0.66	179	0.53	2.49
4	644	0.84	208	0.60	2.89
5	618	0.79	162	0.47	2.26
6	616	0.85	168	0.46	2.06
基质					
7	603	0.94	178	0.44	2.10
8	597	0.63	196	0.80	2.31
9	611	0.79	131	0.36	1.67
10	630	0.59	168	0.48	2.00
11	615	0.69	151	0.41	1.82
12	614	0.80	147	0.39	1.73
13	611	0.77	146	0.39	1.78
14	637	0.84	149	0.38	1.80
15	632	0.71	144	0.40	1.78
16	643	0.51	147	0.43	1.71
17	632	0.53	147	0.42	1.64
18	612	0.94	152	0.71	1.74

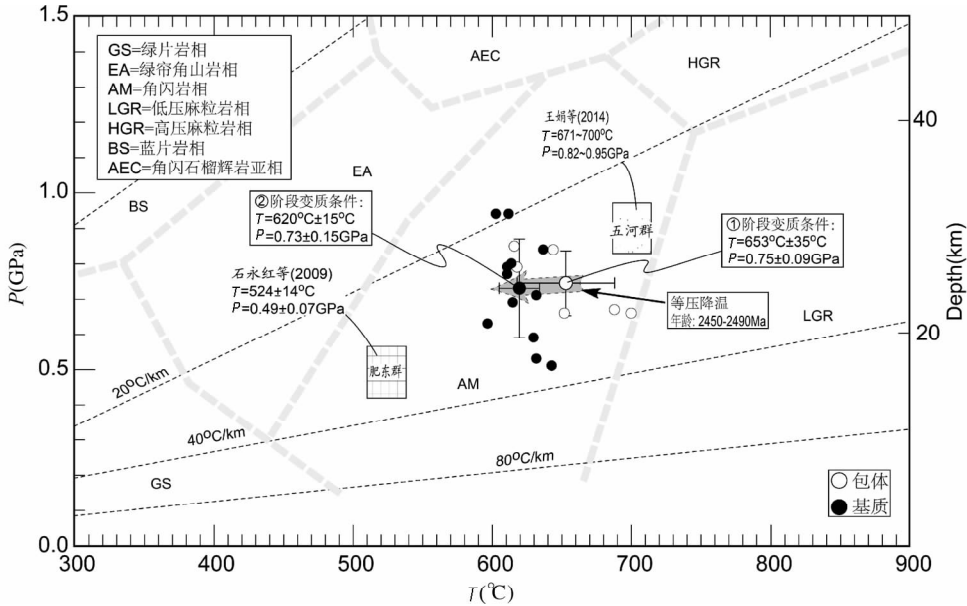


图5 磁铁石榴角闪岩峰期变质  $P$ - $T$  条件图

Fig.5 Plot of metamorphic peak  $P$ - $T$  conditions of the magnetite garnet amphibole

- 1)  $10py + 21fact = 10gr + 15grun + 6tr$
- 2)  $4parg + 12q = 2gr + cumm + ts + 2gl$
- 3)  $42parg + 114q = 14py + 28gr + 9cumm + 21gl + 12H_2O$
- 4)  $7alm + 12parg + 36q = 7py + 6gr + 3grun + 3ts + 6gl$
- 5)  $12parg + 36q = 2py + 4gr + 3tr + 3ts + 6gl$
- 6)  $3py + 14gr + 3grun + 12q + 12mt = 11alm + 12andr + 3ts$

从图5可以看出,①阶段的温压范围为:  $T = 616 \sim 700^\circ\text{C}$  和  $P = 0.66 \sim 0.85\text{GPa}$ , 平均温压为  $\bar{T} = 653 \pm 35^\circ\text{C}$  和  $\bar{P} = 0.75 \pm 0.09\text{GPa}$ 。②阶段的温压范围为:  $T = 597 \sim 643^\circ\text{C}$  和  $P = 0.51 \sim 0.94\text{GPa}$ , 平均温压为  $\bar{T} = 620 \pm 15^\circ\text{C}$  和  $\bar{P} = 0.73 \pm 0.15\text{GPa}$ 。两者均处于角闪岩相范围。根据平均的  $P$ - $T$  条件的变化大致可以看出,①阶段→②阶段显示了一个轻微的等压降温演化过程。然而,如果考虑到温压误差或温压变化范围,这两阶段的变质条件应该十分接近,并且从成分变化方面(图3),①阶段和②阶段矿物没有显著差异,这也许暗示了由①阶段到②阶段可能是一个快速或短暂的过程,应于同一期变质条件下形成(于振清等, 2009),从而导致温度差异并不明显。

对比石永红等(2009)对肥东群的研究,本次磁铁石榴角闪岩的变质条件明显高于他们的结果,但接近于王娟等(2014)确定的华北板块的东部陆块中的五河群变质条件。结合确定的变质年龄 2450~2490Ma(见后述)和等压降温  $P$ - $T$  样式分析(图5、图6g),该类岩石变质特征十分类似 Zhao and Zhai (2013)确定的 2.5Ga 变质事件和演化过程。换言之,该岩石可能源于华北板块。

## 5 锆石 U-Pb 定年

本次对磁铁石榴角闪岩(样品 TF001-2)进行了锆石 U-

Pb 定年。锆石单矿物挑选工作由河北省地勘局廊坊实验室完成,样品重约 15kg,共挑选出约 200 单颗锆石。锆石制靶由合肥工业大学 LA-ICPMS 洁净实验室完成,锆石阴极发光(CL)照相由桂林理工大学电子探针实验室完成,仪器型号 XM-Z09013TPCL。锆石 U-Pb 定年分析由合肥工业大学 LA-ICPMS 实验室完成,实验条件:激光器工作频率为 10Hz,其中激光剥蚀束斑为  $32\mu\text{m}$ ,信号有效采集时间为 50s,每分析测试 5 个样品点测两次标准锆石 91500。锆石数据处理采用 ICPMSDateCal7.5 软件(Ludwing, 2003)和 ISOPLLOT 程序,单个测点同位素年龄的误差为  $1\sigma$ ,加权平均年龄具有 95% 置信度。此外,锆石中矿物包体的测定由中国科学技术大学地球和空间科学学院拉曼实验室分析完成,仪器型 Thermo Fisher DXR。年龄分析数据见表 3。

根据显微镜下的透、反射光的研究,样品 TF001-2 中的锆石多为浑圆状或短柱状,自形程度较低,粒径  $50 \sim 300\mu\text{m}$ ,长宽比为  $2:1 \sim 1:1$ 。CL 图像显示,锆石多为斑杂状分带、面状结构、云雾状分带,无震荡环带(图 6a-c)。此外,这些锆石常具有较多的矿物包体,拉曼光谱分析显示这些包体多为角闪石和磷灰石(图 6a-d)。

由于锆石粒径相对较小和激光剥蚀束斑较大的原因,本次锆石 U-Pb 定年仅获得了 40 个数据点,其中 3 个数据点为谐和年龄,其余数据点为不谐和年龄(表 3)。3 个谐和年龄的锆石的 Th/U 比值分别为 0.09、0.11 和 0.15,基本上小于或约等于 0.1,年龄分别是  $2473 \pm 15\text{Ma}$ 、 $2490 \pm 18\text{Ma}$  和  $2450 \pm 15\text{Ma}$ ,加权平均年龄为  $2469 \pm 49\text{Ma}$  (MSWD = 1.5,  $n = 3$ ) (图 6g)。而 37 个不谐和年龄的锆石的 Th/U 比值 0.1~0.4 (多为 0.1),其年龄范围为 2350~2490Ma,均位于不协和线上,上交点年龄为  $2458 \pm 25\text{Ma}$ (图 6g)。结合 CL 图像分析,

表3 样品 TF001-2 锆石 U-Pb 定年分析数据

Table 3 The zircon U-Pb date of the sample TF001-2

测点号	<sup>232</sup> Th (×10 <sup>-6</sup> )	<sup>238</sup> U (×10 <sup>-6</sup> )	Th/U	<sup>206</sup> Pb (×10 <sup>-6</sup> )	同位素年龄(Ma)						同位素比值					
					<sup>207</sup> Pb/ <sup>206</sup> Pb		<sup>207</sup> Pb/ <sup>235</sup> U		<sup>206</sup> Pb/ <sup>238</sup> U		<sup>207</sup> Pb/ <sup>206</sup> Pb		<sup>207</sup> Pb/ <sup>235</sup> U		<sup>206</sup> Pb/ <sup>238</sup> U	
					1σ	1σ	1σ	1σ	1σ	1σ	1σ	1σ	1σ	1σ		
1	40.9	198	0.2065	96.90	2414	11	2261	14	2093	11	0.1561	0.0010	8.2655	0.1310	0.3835	0.0024
2	10.4	109	0.0961	51.82	2422	16	2265	14	2093	10	0.1569	0.0014	8.3066	0.1258	0.3836	0.0021
3	12.9	95.3	0.1356	44.66	2456	17	2246	14	2031	13	0.1589	0.0017	8.1346	0.1264	0.3704	0.0028
4	31.6	159	0.1993	75.95	2439	14	2266	13	2077	13	0.1584	0.0013	8.3180	0.1173	0.3802	0.0028
5	19.8	184	0.1072	83.34	2439	13	2227	13	1997	10	0.1584	0.0012	7.9637	0.1167	0.3631	0.0022
6	20.2	128	0.1576	43.54	2358	18	1936	15	1563	15	0.1510	0.0015	5.7339	0.0964	0.2744	0.0029
7	57.1	263	0.2169	112.1	2398	10	2142	10	1879	7	0.1547	0.0009	7.2476	0.0841	0.3383	0.0014
8	65.5	225	0.2912	111.9	2439	10	2293	11	2127	9	0.1583	0.0009	8.5654	0.1050	0.3908	0.0020
9	35.1	159	0.2208	63.91	2394	16	2090	13	1791	9	0.1542	0.0014	6.8318	0.0975	0.3202	0.0019
10	37.3	196	0.1903	83.82	2405	11	2171	13	1925	8	0.1553	0.0011	7.4798	0.1045	0.3479	0.0017
11	52.6	255	0.2060	92.76	2350	12	1992	13	1662	10	0.1502	0.0010	6.1099	0.0887	0.2942	0.0019
12	27.3	197	0.1384	81.84	2350	12	2113	13	1876	8	0.1502	0.0010	7.0157	0.1021	0.3378	0.0017
13	27.2	165	0.1650	73.72	2388	17	2189	15	1979	10	0.1538	0.0016	7.6382	0.1299	0.3594	0.0022
14	19.7	141	0.1395	62.93	2381	13	2190	16	1987	13	0.1531	0.0011	7.6397	0.1351	0.3611	0.0026
15	65.4	237	0.2763	111.7	2416	11	2221	16	2012	9	0.1563	0.0010	7.9100	0.1439	0.3662	0.0019
16	13.7	107	0.1289	48.57	2422	15	2250	19	2060	20	0.1568	0.0014	8.1675	0.1715	0.3766	0.0044
17	30.0	224	0.1341	98.34	2388	11	2195	16	1991	15	0.1537	0.0010	7.6829	0.1376	0.3618	0.0032
18	25.8	233	0.1104	101.73	2361	12	2164	14	1959	7	0.1514	0.0011	7.4266	0.1145	0.3551	0.0016
19	50.5	373	0.1352	139.4	2416	10	2052	14	1706	8	0.1563	0.0009	6.5482	0.1037	0.3030	0.0017
20	25.4	231	0.1099	90.48	2389	211	2106	17	1823	17	0.1538	0.0010	6.9581	0.1366	0.3268	0.0036
21	10.1	110	0.0925	55.39	2473	15	2378	17	2265	14	0.1616	0.0014	9.4049	0.1718	0.4210	0.0032
22	16.6	116	0.1431	48.97	2403	17	2156	16	1902	12	0.1551	0.0015	7.3587	0.1345	0.3432	0.0025
23	24.1	208	0.1155	90.27	2369	8	2171	14	1965	8	0.1520	0.0012	7.4814	0.1174	0.3563	0.0016
24	10.1	89.5	0.1134	46.27	2490	18	2387	16	2267	12	0.1633	0.0017	9.4970	0.1672	0.4215	0.0027
25	10.4	111	0.0931	50.80	2453	19	2271	17	2070	13	0.1598	0.0013	8.3658	0.1579	0.3787	0.0027
26	52.9	227	0.2325	103.7	2406	11	2209	17	2001	11	0.1552	0.0010	7.8029	0.1449	0.3639	0.0023
27	12.1	105	0.1157	46.89	2417	-184	2240	22	2038	26	0.1564	0.0015	8.0769	0.1988	0.3719	0.0056
28	31.4	159	0.1978	64.85	2377	17	2107	14	1839	9	0.1528	0.0014	6.9639	0.1121	0.3301	0.0018
29	11.5	97.1	0.1182	48.28	2484	15	2350	15	2193	12	0.1627	0.0014	9.1185	0.1515	0.4052	0.0025
30	13.0	105	0.1247	50.50	2450	18	2292	16	2116	16	0.1595	0.0017	8.5596	0.1546	0.3885	0.0034
31	16.0	117	0.1373	52.16	2383	15	2201	15	2006	8	0.1532	0.0013	7.7421	0.1251	0.3651	0.0018
32	42.8	243	0.1763	92.77	2444	12	2083	15	1732	12	0.1589	0.0012	6.7810	0.1122	0.3082	0.0025
33	16.1	109	0.1481	55.88	2450	15	2361	14	2258	11	0.1593	0.0014	9.2289	0.1382	0.4194	0.0025
34	23.1	148	0.1563	69.23	2455	15	2302	16	2128	20	0.1600	0.0014	8.6488	0.1499	0.3912	0.0044
35	28.1	191	0.1471	80.92	2389	14	2160	13	1933	8	0.1529	0.0012	7.3922	0.1085	0.3497	0.0017
36	105	269	0.3899	126.1	2408	20	2214	14	2006	10	0.1556	0.0013	7.8527	0.1189	0.3651	0.0021
37	13.1	102	0.1290	46.57	2410	16	2257	17	2085	20	0.1558	0.0014	8.2367	0.1543	0.3819	0.0043
38	13.9	148	0.0940	51.30	2376	17	2010	17	1662	12	0.1525	0.0015	6.2426	0.1196	0.2941	0.0023
39	27.3	189	0.1444	85.33	2398	21	2199	17	1987	14	0.1547	0.0019	7.7164	0.1421	0.3610	0.0029
40	30.1	147	0.2051	66.40	2413	12	2219	15	2009	14	0.1559	0.0011	7.8897	0.1298	0.3657	0.0030

注:测点 21、24、30 三组数据为锆石谐和年龄数据

这些锆石应均为变质锆石(吴元保和郑永飞, 2004),故它们的年龄代表的是变质年龄。尽管,这里的上交点年龄并不能准确再现该变质事件的精确年龄,但其具有重要的参考价值。参照 3 个谐和年龄来看(图 6g),上交点年龄与其十分类同,这意味着 3 个谐和年龄应该能较为确切地反映某一变质事件年龄。参照 Gebauer *et al.* (1997)、Hermann *et al.*

(2001)、吴元保和郑永飞(2004)、Liu *et al.* (2004, 2011)、Liu *et al.* (2007) 和 Zheng (2008) 的研究,并根据此次拉曼光谱和定年分析结果,我们认为这 3 个谐和年龄反映的是①和②阶段变质作用年龄,因为这 3 个年龄均是在含角闪石和磷灰石矿物包裹体附近区域获得的(图 6a-d),而这些包体在①和②阶段变质矿物组合均普遍发育。



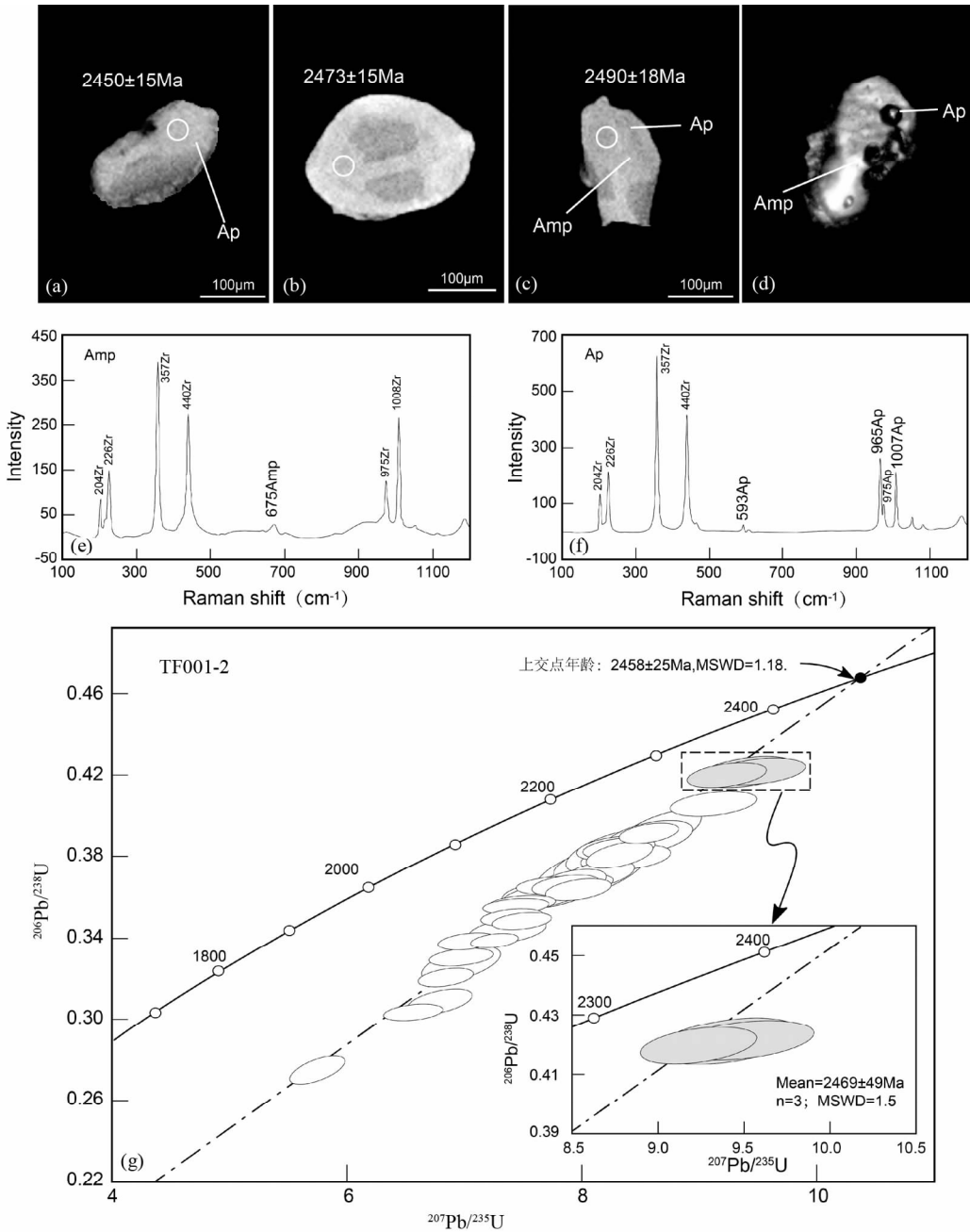


图6 样品 TF001-2 锆石 CL 图、包体拉曼光谱及 U-Pb 定年谐和图

Fig. 6 CL image, Raman spectra and concordia plots of zircons from sample TF001-2

## 6 磁铁石榴角闪岩构造归属讨论

目前,人们普遍认同郯庐断裂(安徽段)是华北和扬子板块的重要边界断裂,其左旋走滑错距长达 >500km。主断裂严格地呈狭窄的线性条带发育于扬子板块内(Xu *et al.*, 1987; Zhu *et al.*, 2005, 2009, 2010; Zhang *et al.*, 2007, 2013a, b; 朱光等, 2009; 赵田等, 2014), 出露的宽度 ~5km (图 1), 而华北板块并未受到郯庐断裂明显的改造和影响。

换言之, 郯庐断裂带内的物质均由扬子板块构成, 没有任何源于华北板块的物质。

通常认为华北和扬子板块的物质差异主要体现在年龄方面。Zhao and Zhai (2013) 的研究表明, 华北板块最终拼合在 1.85Ga 完成, 其内部出露有极少量的始太古 (3.8 ~ 3.6Ga) 岩石地块和部分 2.8 ~ 2.7Ga 初生陆壳。并强调华北板块主体是由 2.6 ~ 2.5Ga 高级片麻岩和低-中级花岗岩-绿岩构成, 同时指出在 ~2.5Ga 时期, 华北东、西部陆块普遍经历了绿片岩相至麻粒岩相的逆时针等压降温变质作用, 反映

了源于地幔岩浆的底侵作用过程(Zhao *et al.*, 1998, 1999a, b; Zhao and Zhai, 2013)。而 1.95 ~ 1.85Ga 变质年龄则反映了华北板块上西部、中部和东部陆块的彼此之间碰撞俯冲时限。具体到郯庐断裂西侧的华北东部陆块(图 1 中的插图), Zhao and Zhai (2013) 认为该陆块在 2.2 ~ 1.9Ga 形成陆内裂谷(张秋生, 1988; Li *et al.*, 2004, 2005, 2006), 形成长gang 和 Nangrim 2 个块体, 并于 1.9Ga 时间俯冲碰撞拼合完成。相比较而言, 扬子板块的岩石年龄具有较广的年龄范围, 根据前人的研究其大致可分为 7 个年龄区间 3.3 ~ 2.9Ga, 2.7 ~ 2.5Ga, 2.0 ~ 1.7Ga, ~ 1.0Ga, 850 ~ 650Ma, 480 ~ 400Ma 和 245 ~ 200Ma(Hacker *et al.*, 1998, 2006; Qiu *et al.*, 2000; Ratschbacher *et al.*, 2003, 2006; Wu *et al.*, 2004; Zheng *et al.*, 2007, 2008; Chen *et al.*, 2003, 2009; Zhang *et al.*, 2006; 郑永飞和张少兵, 2007; Gao *et al.*, 2011; 魏君奇等, 2012), 其中后三个年龄范围在扬子板块内普遍发育, 而前三个较老的年龄在扬子板块上出露极少, 且 2.7 ~ 2.5Ga 反映的是角闪岩相的变质事件。

对比本次张八岭隆起区的肥东群中的磁铁石榴角闪岩的年代学和变质岩石学的研究来看, 磁铁石榴角闪岩中的 3 颗变质锆石的谐和年龄在 2450 ~ 2490Ma, 加权平均年龄为 2496 ± 49Ma, 其十分接近于华北板块的 ~ 2.5Ga 的变质年龄。而其他 37 颗变质锆石的不谐和年龄变化也较为单一, 基本上在 2350 ~ 2484Ma 范围(表 3), 这暗示了该岩石类型可能源于华北板块。然而, 根据 Qiu *et al.* (2000) 和魏君奇等(2012) 的研究, 该年龄也同样落入扬子板块的 2.7 ~ 2.5Ga 的范围, 似乎该岩石具扬子板块的亲缘性。对此, 本文没有较为明确的结论。这里也许可以假设两种情形: (1) 磁铁石榴角闪岩属于华北板块物质, 由于郯庐断裂的左旋走滑作用, 其呈构造透镜体的形式被卷入郯庐断裂带内; (2) 该岩石本身就归属于扬子板块, 可能是郯庐断裂带(安徽段)内出露的最老的岩石。

然而, 结合地质背景、构造地质学和变质岩石学的研究, 本次研究更倾向于前一种认识。主要理由是: (a) 从地质背景来看, 磁铁石榴角闪岩在华北东部陆块(安徽段)的五河杂岩和霍邱群中广泛发育该类岩石(安徽省地质矿产局, 1987; 杨晓勇等, 2012), 而安徽境内的扬子板块则没有这类相关类型岩石的确证。这暗示了该类岩石可能的物源来自于华北板块; (b) 在年龄变化方面, 磁铁石榴角闪岩的年龄十分单一, 基本在 ~ 2.5Ga 时间段(表 1), 缺乏任何类似于扬子板块的较为年轻的年龄(850 ~ 650Ma, 480 ~ 400Ma 和 245 ~ 200Ma)。且该年龄十分接近郯庐断裂西侧华北东部陆块的年龄(Liu *et al.*, 2009; 许文良等, 2006; 杨晓勇等, 2012; 图 1 中插图), 这从另一个侧面反映了该岩石具华北板块亲缘性; (c) 从变质 *P-T* 演化来看, 磁铁石榴角闪岩显示了轻微的等压降温特征(图 5), 与 Zhao and Zhai (2013) 阐述的华北东、西部陆块在 ~ 2.5Ga 发生的源于地幔岩浆的底侵事件十分吻合。此外, 该岩石的变质 *P-T* 条件也十分类似于五河群

中石榴角闪岩的变质条件(王娟等, 2014), 明显不同于肥东群的变质条件(王永红等, 2009); (d) 构造地质学分析显示, 磁铁石榴角闪岩及其围岩是呈构造透镜体产于变形的花岗岩之中, 周边被糜棱岩所限定(图 1b)。其面理和线理与郯庐断裂带中韧性剪切带的面理和线理呈大角度相交, 暗示了其可能为一个外来的构造块体, 并非原地物质。基于本次研究的结果, 我们认为张八岭隆起区的肥东群中的磁铁石榴角闪岩可能来源于华北板块, 由于郯庐断裂的左旋走滑作用被构造并置于扬子板块中。进一步地, 可以推测郯庐断裂东侧界限位于方集-蛮山口以东的全椒盆地中, 结合赵田等(2014) 研究可以看出, 该断裂在横向上(安徽段)的宽度至少在 10 ~ 15km 范围(图 1)。

**致谢** 感谢朱光教授在本文撰写过程中的支持与帮助; 感谢吴春明教授和林伟研究员对本文的审阅及意见。

## References

- Bureau of Geology and Mineral Resources of Anhui Province. 1987. Regional Geology of Anhui Province. Beijing: Geological Publishing House (in Chinese)
- Chang EZ. 1996. Collisional orogene between North and South China and its eastern extension in the Korean Peninsula. *Journal of Southeast Asian Earth Sciences*, 13(3-5): 267-277
- Chen FK, Guo JH, Jiang LL, Siebel W, Cong B and Satir M. 2003. Provenance of the Beihuaiyang lower-grade metamorphic zone of the Dabie ultrahigh-pressure collisional orogen, China: Evidence from zircon ages. *Journal of Asian Earth Sciences*, 22(4): 343-352
- Chen FK, Zhu XY, Wang W, Wang F, Hieu PT and Siebel W. 2009. Single-grain detrital muscovite Rb-Sr isotopic composition as an indicator of provenance for the Carboniferous sedimentary rocks in northern Dabie, China. *Geochemical Journal*, 43(4): 257-273
- Chung SL. 1999. Trace element and isotope characteristics of Cenozoic basalts around the Tanlu fault with implications for the eastern plate boundary between North and South China. *The Journal of Geology*, 107(3): 301-312
- Droop GTB. 1987. A general equation for estimating  $Fe^{3+}$  concentrations in ferromagnesian silicates and oxides from microprobe analyses, using stoichiometric criteria. *Mineralogical Magazine*, 51: 431-435
- Gao S, Jie Y, Zhao L, Li M, Hu ZC, Guo JL, Yuan HL, Gong HJ, Xiao GG and Wei JQ. 2011. Age and growth of the Archean Kongling terrain, South China, with emphasis on 3.3Ga granitoid gneisses. *American Journal of Science*, 311(2): 1-30
- Gebauer D, Schertl HP, Brix M and Schreyer W. 1997. 35Ma old ultrahigh-pressure metamorphism and evidence for very rapid exhumation in the Dora Maira Massif, Western Alps. *Lithos*, 41(1): 5-24
- Gilder SA, Leloup PH, Courtillot V, Chen Y, Coe RS, Zhao XX, Halim WN, Cogne JP and Zhu R. 1999. Tectonic evolution of the Tancheng-Lujiang (Tan-Lu) fault via Middle Triassic to Early Cenozoic paleomagnetic data. *Journal of Geophysical Research*, 104(B7): 15365-15390
- Hacker BR, Ratschbacher L, Webb L, Ireland T, Walker D and Shuwen D. 1998. U/Pb zircon ages constrain the architecture of the ultrahigh-pressure Qinling-Dabie Orogen, China. *Earth and Planetary Science Letters*, 161(1): 215-230
- Hacker BR, Wallis SR, Ratschbacher L, Grove M and Gehrels G. 2006. High-temperature geochronology constraints on the tectonic history and architecture of the ultrahigh-pressure Dabie-Sulu Orogen.

- Tectonics, 25(5), doi: 10.1029/2005TC001937
- Hammarstrom JM and Zen E. 1986. Aluminum in hornblende: An empirical geobarometer. *American Mineralogist*, 71(11–12): 1297–1313
- Hermann J, Rubatto D, Korsakov A and Shatsky V. 2001. Multiple zircon growth during fast exhumation of diamondiferous, deeply subducted continental crust (Kokchetav Massif, Kazakhstan). *Contributions to Mineralogy and Petrology*, 141(1): 66–82
- Holland T, Baker J and Powell R. 1998. Mixing properties and activity-composition and relationships of chlorites in the system MgO-FeO-Al<sub>2</sub>O<sub>3</sub>-SiO<sub>2</sub>-H<sub>2</sub>O. *European Journal of Mineralogy*, 10(3): 395–406
- Hollister LS, Grisson GC, Peters EK, Stowell HH and Sisson VB. 1987. Confirmation of the empirical correlation of aluminum in hornblende with pressure of solidification of calc-alkaline pluton. *American Mineralogist*, 72(3–4): 231–239
- Hsu KJ, Li J, Chen I, Wang Q and Sun S. 1987. Tectonic evolution of Qinling Mountains, China. *Eclogae Geol. Helv.*, 80: 735–752
- Johnson W and Rutherford MJ. 1989. Experimental calibration of the aluminum-in hornblende geobarometer with application to Long Valley Caldera (California) volcanic rocks. *Geology*, 17(9): 837–841
- Kang T, Liu XY, Wang J, Nie F and Shi YH. 2013. Analysis of metamorphic attribution and geochronology for the Feidong terrane in the east of the Tan-Lu Fault. *Acta Petrologica Sinica*, 29(9): 3142–3158 (in Chinese with English abstract)
- Li SZ, Zhao GC, Sun M, Wu FY, Liu JZ, Hao DF, Han ZZ and Luo Y. 2004. Mesozoic, not Paleoproterozoic SHRIMP U-Pb zircon ages of two Liaoji granites, Eastern Block, North China Craton. *International Geology Review*, 46(2): 162–176
- Li SZ, Zhao GC, Sun M, Wu FY, Hao DF, Han ZZ, Luo Y and Xia XP. 2005. Deformation history of the Paleoproterozoic Liaohu assemblage in the Eastern Block of the North China Craton. *Journal of Asian Earth Sciences*, 24(5): 654–674
- Li SZ, Zhao GC, Sun M, Han ZZ, Zhao GT and Hao DF. 2006. Are the South and North Liaohu Groups of the North China Craton different exotic terranes? Nd isotope constraints. *Gondwana Research*, 9(1–2): 198–208
- Li ZX. 1994. Collision between the north and south blocks: A crustal detachment model for suturing in the region east of the Tan-Lu fault. *Geology*, 22(8): 739–742
- Lin JL and Fuller M. 1990. Paleomagnetism, North and South China collision, and the Tan-Lu fault. *Philosophy Transaction of Royal Society of London A*, 331(1620): 589–598
- Lin SF and Li ZX. 1995. Collision between the North and South China blocks: A crustal-detachment model for suturing in the region east of the Tanlu fault; Comment. *Geology*, 23(6): 574–575
- Lin W, Faure M, Wang QC, Monié P and Panis D. 2005. Triassic polyphase deformation in the Feidong-Zhangbaling Massif (Eastern China) and its place in the collision between the North China and South China Blocks. *Journal of Asia Earth Sciences*, 25(1): 121–136
- Lin W, Shi YH and Wang QC. 2009. Exhumation tectonics of the HP-UHP orogenic belt in eastern China: New structural-petrological insights from the Tongcheng massif, eastern Dabie Shan. *Lithos*, 109(3–4): 285–303
- Liu FL, Xu ZQ, Liou JG and Song B. 2004. SHRIMP U-Pb ages of ultrahigh-pressure and retrograde metamorphism of gneisses, southwestern Sulu terrane, eastern China. *Journal of Metamorphic Geology*, 22(4): 315–326
- Liu FL and Liou JG. 2011. Zircon as the best mineral for *P-T*-time history of UHP metamorphism: A review on mineral inclusions and U-Pb SHRIMP ages of zircons from the Dabie-Sulu UHP rocks. *Journal of Asian Earth Sciences*, 40(1): 1–39
- Liu YC, Li SG and Xu ST. 2007. Zircon SHRIMP U-Pb dating for gneisses in northern Dabie high *T/P* metamorphic zone, central China; Implications for decoupling with subducted continental crust. *Lithos*, 96(1): 170–185
- Liu YC, Wang AD, Rolfo F, Groppo C, Gu XF and Song B. 2009. Geochronological and petrological constraints on Palaeoproterozoic granulite facies metamorphism in southeastern margin of the North China Craton. *Journal of Metamorphic Geology*, 27(2): 125–138
- Ludwig KR. 2003. *User's Manual for Isoplot/Exersion 3.00*; A Geochronological Toolkit for Microsoft Excel. Berkeley Geochronology Center; Special Publication, 4: 1–70
- Meng QR, Li SY and Li RW. 2007. Mesozoic evolution of the Hefei basin in eastern China: Sedimentary response to deformations in the adjacent Dabie Shan and along the Tanlu fault. *Geological Society of America Bulletin*, 119(7–8): 897–916
- Niu ML, Zhu G, Liu GS, Wang DX and Song CZ. 2002. Tectonic setting and deep processes of Mesozoic magmatism in middle-south segment of the Tan-Lu fault. *Chinese Journal of Geology*, 37(4): 393–404 (in Chinese with English abstract)
- Niu ML, Zhu G, Liu GS and Song CZ. 2005. Correlation studies of rare earth elements in syntectonic intrusions of strike-slip stage along southern segment of Tanlu Fault Zone. *Journal of The Chinese Rare Earth Society*, 23(2): 235–238 (in Chinese with English abstract)
- Niu ML. 2006. <sup>40</sup>Ar/<sup>39</sup>Ar dating of biotite from the Mesozoic intrusions in Zhangbaling area and its geological significance. *Chinese Journal of Geology*, 41(2): 217–225 (in Chinese with English abstract)
- Okay AI and Sengor AMC. 1992. Evidence for intracontinental thrust related exhumation of the ultra-high-pressure rocks in China. *Geology*, 20(5): 411–414
- Powell R and Holland TJB. 2008. On thermobarometry. *Journal of Metamorphic Geology*, 26(2): 155–179
- Qiu YM, Gao S, McNaughton NJ, Groves DI and Ling WL. 2000. First evidence of >3.2Ga continental crust in the Yangtze craton of south China and its implications for Archean crustal evolution and Phanerozoic tectonics. *Geology*, 28(1): 11–14
- Ratschbacher L, Hacker BR, Calvert A, Webb LE, Grimmer JC, McWilliams MO, Ireland T, Dong SW and Hu JM. 2003. Tectonics of the Qinling (Central China): Tectonostratigraphy, geochronology, and deformation history. *Tectonophysics*, 366(1): 1–53
- Ratschbacher L, Franz L, Enkelmann E, Jonckheere R, Hacker BR, Dong SW and Zhang YQ. 2006. The Sino-Korean-Yangtze suture, the Huwan detachment, and the Paleozoic-Tertiary exhumation of (ultra) high-pressure rocks along the Tongbai-Xinxian-Dabie Mountains. *Geological Society of America*, 403: 43–75
- Schmid JC, Ratschbacher L, Hacker BR, Gaitzsch I and Dong SW. 1999. How did the foreland react? Yangtze foreland fold-and-thrust belt deformation related to exhumation of the Dabie Shan ultrahigh-pressure continental crust (eastern China). *Terra Nova*, 11(6): 266–272
- Schmidt MW. 1992. Amphibole composition in tonalite as a function of pressure: An experimental calibration of the Al-in-hornblende barometer. *Contrib. Mineral. Petrol.*, 110(2–3): 304–310
- Shi YH, Zhu G and Wang DX. 2009. Metamorphic *P-T* evolution for the garnet amphibolite from Feidong Group in the south of Zhangbaling uplift across Tan-Lu fault and its influence on tectonics. *Acta Petrologica Sinica*, 25(12): 3335–3345 (in Chinese with English abstract)
- Wan TF and Zhu H. 1996. The maximum sinistral strike-slip and its forming age of Tancheng-Lujiang fault zone. *Geological Journal of Universities*, 2(1): 14–27 (in Chinese with English abstract)
- Wang EC, Meng QR, Burchfiel BC and Zhang GW. 2003. Mesozoic large-scale lateral extrusion, rotation, and uplift of the Tongbai-Dabie Shan belt in East China. *Geology*, 31(4): 307–310
- Wang J, Huang B, Pu XP, Kang T and Shi YH. 2014. The investigation on metamorphic petrology and *P-T* conditions of Wuhe complex rocks: Evidences from Drill ZK02 in the south of Mengcheng area. *Chinese Journal of Geology*, 49(2): 556–575 (in Chinese with English abstract)
- Wang XF, Li ZG, Chen BL, Zhang Q, Chen XH, Xing LS, Chen ZL, Dong SW and Wu HM. 1998. Formation and evolution of the Tan-Lu strike-slip fault system and its geological significance. In: Zheng YD (ed.). *Proceedings of 30<sup>th</sup> International Geological Congress*, Vol.

14. Beijing: Geological Publishing House, 176 – 196 (in Chinese with English abstract)
- Wang YS, Zhu G, Liu GS and Wang DX. 2004. Evolution of sericite polytype and crystallinity during mylonitization: Examples from the southern part of Tan-Lu fault zones. *Acta Petrologica Sinica*, 20 (6): 1485 – 1492 (in Chinese with English abstract)
- Wang YS and Zhu G. 2005. Cooling and deformation ages in  $^{40}\text{Ar}/^{39}\text{Ar}$  dating. *Geological Bulletin of China*, 24 (3): 285 – 290 (in Chinese with English abstract)
- Wang YS, Zhu G, Chen W, Song CZ and Liu GS. 2005. Thermochronologic information from the Tan-Lu fault zone and its relationship with the exhumation of the Dabie Mountains. *Geochimica*, 34(3): 193 – 215 (in Chinese with English abstract)
- Wang YS, Zhu G, Song CZ, Liu GS, Xiang BW, Li CC and Xie CL. 2006.  $^{40}\text{Ar}-^{39}\text{Ar}$  geochronology records of transition from strike-slip to extension in the Tan-Lu fault zone on eastern terminal of the Dabie Mountains. *Chinese Journal of Geology*, 41 (2): 242 – 255 (in Chinese with English abstract)
- Watson MP, Hayward AB and Parkinson DN. 1987. Plate tectonics history, basin development and petroleum source rock deposition onshore China. *Marine and Petroleum Geology*, 4(3): 205 – 225
- Wei CJ and Shan ZG. 1997. Metamorphism of the Susong complex from the southern Dabie Mountains, Anhui Province. *Acta Petrologica Sinica*, 13(3): 356 – 368 (in Chinese with English abstract)
- Wei JQ and Wang JX. 2012. Zircon age and Hf isotope compositions of amphibolite enclaves from the Kongling complex. *Geological Journal of China Universities*, 18(4): 589 – 600 (in Chinese with English abstract)
- Whitney DL and Evans BW. 2010. Abbreviations for names of rock-forming minerals. *American Mineralogist*, 95(1): 185 – 187
- Worley B and Powell R. 2000. High-precision relative thermobarometry: Theory and a worked example. *Journal of Metamorphic Geology*, 18 (1): 91 – 102
- Wu CM, Zhang J and Ren LD. 2004. Empirical garnet-biotite-plagioclase-quartz (GBPQ) geobarometry in medium- to high-grade metapelites. *Journal of Petrology*, 45(9): 1907 – 1921
- Wu YB and Zheng YF. 2004. Genesis of zircon and its constraints on interpretation of U-Pb age. *Chinese Science Bulletin*, 49(16): 1589 – 1604 (in Chinese)
- Xu JW. 1980. The great left-lateral horizontal displacement of Tancheng-Lujiang fault zone, eastern China. *Journal of Hefei Polytechnic University (Natural Science)*, (1): 1 – 26 (in Chinese with English abstract)
- Xu JW, Zhu G, Tong WX, Cui KR and Liu Q. 1987. Formation and evolution of the Tancheng-Lujiang wrench fault system; A major shear system to the northern of the Pacific Ocean. *Tectonophysics*, 134(4): 273 – 310
- Xu JW and Zhu G. 1994. Tectonic models of the Tan-Lu fault zone, eastern China. *International Geology Review*, 36(8): 771 – 784
- Xu WL, Yang DB, Pei FP, Yang CH, Liu XM and Hu ZC. 2006. Age of the Wuhe complex in the Bengbu uplift: Evidence from LA-ICP-MS zircon U-Pb dating. *Geology in China*, 33(1): 132 – 137 (in Chinese with English abstract)
- Yang XY, Wang BH, Du ZB, Wang QC, Wang YX, Tu ZB, Zhang WL and Sun WD. 2012. On the metamorphism of the Huoqiu Group, forming ages and mechanism of BIF and iron deposit in the Huoqiu region, southern margin of North China craton. *Acta Petrologica Sinica*, 28(11): 3476 – 3496 (in Chinese with English abstract)
- Yin A and Nie SY. 1993. An indentation model for the North and South China collision and the development of the Tan-Lu and Honam fault systems, eastern Asia. *Tectonics*, 12(4): 801 – 813
- Yu ZQ, Li YX and Xiao LL. 2009. Polymetamorphism, polyphase metamorphism and metamorphic *P-T-t* paths. *Bulletin of Mineralogy, Petrology and Geochemistry*, 28(2): 189 – 194 (in Chinese with English abstract)
- Zhang KJ. 1997. North and South China collision along the eastern and southern North China margins. *Tectonophysics*, 270 (1 – 2): 145 – 156
- Zhang Q, Jim D and Zhu G. 2007. Oblique collision between North and South China recorded in Zhangbaling and Fucha Shan (Dabie-Sulu transfer zone). *The Geology Society America*, 434: 167 – 206
- Zhang Q and Teyssier C. 2013. Flow vorticity in Zhangbaling transpressional attachment zone, SE China. *Journal of Structural Geology*, 48: 72 – 84
- Zhang Q, Giorgis S and Teyssier C. 2013. Finite strain analysis of the Zhangbaling metamorphic belt, SE China: Crustal thinning in transpression. *Journal of Structural Geology*, 49: 13 – 22
- Zhang QS. 1988. Early Crust and Mineral Deposits of Liaodong Peninsula, China. Beijing: Geological Publishing House (in Chinese)
- Zhang SB, Zheng YF, Wu YB, Zhao ZF, Gao S and Wu FY. 2006. Zircon isotope evidence for  $\geq 3.5\text{Ga}$  continental crust in the Yangtze craton of China. *Precambrian Research*, 146(1 – 2): 16 – 34
- Zhang ZM, Liou JG and Coleman RG. 1984. An outline of the plate tectonics of China. *Geol. Soc. Am. Bull.*, 95(3): 295 – 312
- Zhao GC, Wilde SA, Cawood PA and Lu LZ. 1998. Thermal evolution of Archean basement rocks from the eastern part of the North China Craton and its bearing on tectonic setting. *International Geology Review*, 40(8): 706 – 721
- Zhao GC, Wilde SA, Cawood PA and Lu LZ. 1999a. Tectonothermal history of the basement rocks in the western zone of the North China Craton and its tectonic implications. *Tectonophysics*, 310(1 – 4): 37 – 53
- Zhao GC, Cawood PA and Lu LZ. 1999b. Petrology and *P-T* history of the Wutai amphibolites: Implications for tectonic evolution of the Wutai Complex, China. *Precambrian Research*, 93 (2 – 3): 181 – 199
- Zhao GC and Zhai MG. 2013. Lithotectonic elements of Precambrian basement in the North China Craton; Review and tectonic implications. *Gondwana Research*, 23(4): 1207 – 1240
- Zhao T, Zhu G, Lin SZ, Yan LJ and Jiang QQ. 2014. Protolith ages and deformation mechanism of metamorphic rocks in the Zhangbaling uplift segment of the Tan-Lu Fault Zone. *Scientia Sinica (Terrae)*, in press (in Chinese)
- Zheng YF and Zhang SB. 2007. Formation and evolution of Precambrian continental crust in South China. *Chinese Science Bulletin*, 52(1): 1 – 10 (in Chinese)
- Zheng YF, Gao TS, Wu YB, Gong B and Liu XM. 2007. Fluid flow during exhumation of deeply subducted continental crust: Zircon U-Pb age and O-isotope studies of a quartz vein within ultrahigh-pressure eclogite. *Journal of Metamorphic Geology*, 25 (2): 267 – 283
- Zheng YF. 2008. A perspective view on ultrahigh-pressure metamorphism and continental collision in the Dabie-Sulu orogenic belt. *Chinese Science Bulletin*, 53(20): 3081 – 3104
- Zhu G, Xu JW, Liu GS, Li SY and Yu PY. 1998. Tectonic control on development of the foreland basin along the Yangtze River in the Lower Yangtze River region. *Geological Review*, 44(2): 120 – 129 (in Chinese with English abstract)
- Zhu G, Wang DX, Liu GS, Song CZ, Xu JW and Niu ML. 2001. Extensional activities along the Tan-Lu fault zone and its geodynamic setting. *Chinese Journal of Geology*, 36(3): 269 – 278 (in Chinese with English abstract)
- Zhu G, Niu ML, Liu GS, Wang DX and Song CZ. 2002. Structural, magmatic and sedimentary events of the Tan-Lu fault belt during its Early Cretaceous strike-slip movement. *Acta Geologica Sinica*, 76 (3): 325 – 334 (in Chinese with English abstract)
- Zhu G, Liu GS, Niu ML, Song CZ and Wang DX. 2003. Transcurrent movement and genesis of the Tan-Lu fault zone. *Geological Bulletin of China*, 22(3): 200 – 208 (in Chinese with English abstract)
- Zhu G, Wang YS, Niu ML, Liu GS and Xie CL. 2004. Synorogenic movement of the Tan-Lu fault zone. *Earth Science Frontiers*, 11 (3): 169 – 182 (in Chinese with English abstract)
- Zhu G, Wang YS, Liu GS, Niu ML, Xie CL and Li CC. 2005.  $^{40}\text{Ar}/^{39}\text{Ar}$  dating of strike-slip motion on the Tan-Lu Fault Zone, East China. *Journal of Structural Geology*, 27(8): 1379 – 1398

- Zhu G, Xie CL, Wang YS, Niu ML and Liu GS. 2005a. Characteristics of the Tan-Lu high-pressure strike-slip ductile shear zone and its  $^{40}\text{Ar}/^{39}\text{Ar}$  dating. *Acta Petrologica Sinica*, 21(6): 1687–1702 (in Chinese with English abstract)
- Zhu G, Niu ML, Liu GS, Wang YS, Xie CL and Li CC. 2005b.  $^{40}\text{Ar}/^{39}\text{Ar}$  dating for the strike-slip movement on the Feidong part of the Tan-Lu fault belt. *Acta Geologica Sinica*, 79(3): 303–316 (in Chinese with English abstract)
- Zhu G, Wang YS, Wang DX, Niu ML, Liu GS and Xie CL. 2006a. Constraints of foreland sedimentation and deformation on synorogenic motion of the Tan-Lu fault zone. *Chinese Journal of Geology*, 41(1): 102–121 (in Chinese with English abstract)
- Zhu G, Xu YD, Liu GS, Wang YS and Xie CL. 2006b. Structural and deformational characteristics of strike-slip faults along the middle-southern sector of the Tan-Lu fault zone. *Chinese Journal of Geology*, 41(2): 226–241 (in Chinese with English abstract)
- Zhu G, Liu GS, Niu ML, Xie CL, Wang YS and Xiang BW. 2009. Syn-collisional transform faulting of the Tan-Lu Fault Zone, East China. *International Journal of Earth Sciences*, 98(1): 135–155
- Zhu G, Zhang L, Xie CL, Niu ML and Wang YS. 2009. Geochronological constraints on tectonic evolution of the Tan-Lu fault zone. *Chinese Journal of Geology*, 44(4): 1327–1342 (in Chinese with English abstract)
- Zhu G, Niu ML, Xie CL and Wang YS. 2010. Sinistral to normal faulting along the Tan-Lu Fault Zone: Evidence for geodynamic switching of the East China continental margin. *The Journal of Geology*, 118(3): 277–293
- 附中文参考文献**
- 安徽省地质矿产局. 1987. 安徽省区域地质志. 北京: 地质出版社
- 康涛, 刘晓燕, 王娟, 聂峰, 石永红. 2013. 郟庐断裂东侧肥东地块变质属性及年代学研究. *岩石学报*, 29(9): 3142–3158
- 牛漫兰, 朱光, 刘国生, 王道轩, 宋传中. 2002. 郟庐断裂带中-南段中生代岩浆活动的构造背景与深部过程. *地质科学*, 37(4): 393–404
- 牛漫兰, 朱光, 刘国生, 宋传中. 2005. 郟庐断裂带南段走滑期同构造岩体的稀土元素对比研究. *中国稀土学报*, 23(2): 235–238
- 牛漫兰. 2006. 张八岭地区中生代岩体中黑云母的 $^{40}\text{Ar}/^{39}\text{Ar}$ 年龄及其地质意义. *地质科学*, 41(2): 217–225
- 石永红, 朱光, 王道轩. 2009. 郟庐断裂带张八岭隆起南段肥东群石榴角闪岩变质  $P-T$  演化史对其构造属性的制约. *岩石学报*, 25(12): 3335–3345
- 万天丰, 朱鸿. 1996. 郟庐断裂带的最大左行走滑断距及其形成时期. *高校地质学报*, 2(1): 14–27
- 王娟, 黄博, 卜香萍, 康涛, 石永红. 2014. 五河杂岩的变质岩石学及  $P-T$  条件分析——来自蒙城南 ZK02 钻孔的研究. *地质科学*, 49(2): 556–575
- 王小凤, 李中坚, 陈柏林, 张清, 陈宣华, 邢历生, 陈正乐, 董树文, 鄢华梅. 1998. 郟庐走滑断裂系的形成演化及其地质意义. 见: 郑亚东主编. 第30届国际地质大会论文集14. 北京: 地质出版社, 176–196
- 王勇生, 朱光, 刘国生, 王道轩. 2004. 糜棱岩化过程中细粒白云母多型与结晶度的演变——以郟庐断裂带南段为例. *岩石学报*, 20(6): 1485–1492
- 王勇生, 朱光. 2005.  $^{40}\text{Ar}/^{39}\text{Ar}$  测年中的冷却年龄和变形年龄. *地质通报*, 24(3): 285–290
- 王勇生, 朱光, 陈文, 宋传中, 刘国生. 2005. 郟庐断裂带热年代学信息及其与大别造山带折返的关系. *地球化学*, 34(3): 193–215
- 王勇生, 朱光, 宋传中, 刘国生, 向必伟, 李长城, 谢成龙. 2006. 大别山东端郟庐断裂带由走滑向伸展运动转换的 $^{40}\text{Ar}/^{39}\text{Ar}$ 年代学记录. *地质科学*, 41(2): 242–255
- 魏春景, 单振刚. 1997. 安徽省大别山南部宿松杂岩变质作用研究. *岩石学报*, 13(3): 356–368
- 魏君奇, 王建雄. 2012. 崆岭杂岩中斜长角闪岩包体的锆石年龄和 Hf 同位素组成. *高校地质学报*, 18(4): 589–600
- 吴元保, 郑永飞. 2004. 锆石成因矿物学研究及其对 U-Pb 年龄解释的制约. *科学通报*, 49(16): 1589–1604
- 徐嘉伟. 1980. 郟庐断裂带巨大的左行平移运动. *合肥工业大学学报*, (1): 1–26
- 许文良, 杨德彬, 裴福萍, 杨承海, 柳小明, 胡兆初. 2006. 蚌埠隆起区五河杂岩的形成时代: 锆石 LA-ICP-MSU-Pb 定年证据. *中国地质*, 33(1): 132–137
- 杨晓勇, 王波华, 杜贞保, 王启才, 王玉贤, 涂政标, 张文利, 孙卫东. 2012. 论华北克拉通南缘霍邱群变质作用、形成时代及霍邱 BIF 铁矿成矿机制. *岩石学报*, 28(11): 3476–3496
- 于振清, 李艳霞, 肖玲玲. 2009. 多期变质作用、多相变质作用与变质作用  $P-T-t$  轨迹. *矿物岩石地球化学通报*, 28(2): 189–194
- 赵田, 朱光, 林少泽, 严乐佳, 姜芹芹. 2014. 郟庐断裂带张八岭隆起段变质岩的原岩时代与变形机制. *中国科学(地球科学)*, 待刊
- 张秋生. 1988. 辽东半岛早期地壳与矿床. 北京: 地质出版社
- 郑永飞, 张少兵. 2007. 华南前寒武纪大陆地壳的形成和演化. *科学通报*, 52(1): 1–10
- 朱光, 徐嘉伟, 刘国生, 李双应, 虞培玉. 1998. 下扬子地区沿江前陆盆地形成的构造控制. *地质论评*, 44(2): 120–129
- 朱光, 王道轩, 刘国生, 宋传中, 徐嘉伟, 牛漫兰. 2001. 郟庐断裂带的伸展活动及其动力学背景. *地质科学*, 36(3): 269–278
- 朱光, 牛漫兰, 刘国生, 王道轩, 宋传中. 2002. 郟庐断裂带早白垩世走滑运动中的构造、岩浆、沉积事件. *地质学报*, 76(3): 325–334
- 朱光, 刘国生, 牛漫兰, 宋传中, 王道轩. 2003. 郟庐断裂带的平移运动与成因. *地质通报*, 22(3): 200–208
- 朱光, 王勇生, 牛漫兰, 刘国生, 谢成龙. 2004. 郟庐断裂带的同造山运动. *地学前缘*, 11(3): 169–182
- 朱光, 谢成龙, 王勇生, 牛漫兰, 刘国生. 2005a. 郟庐高压走滑韧性剪切带特征及其 $^{40}\text{Ar}/^{39}\text{Ar}$ 定年. *岩石学报*, 21(6): 1687–1702
- 朱光, 牛漫兰, 刘国生, 王勇生, 谢成龙, 李长城. 2005b. 郟庐断裂带肥东段走滑运动的 $^{40}\text{Ar}/^{39}\text{Ar}$ 法定年. *地质学报*, 79(3): 303–316
- 朱光, 王勇生, 王道轩, 牛漫兰, 刘国生, 谢成龙. 2006a. 前陆沉积与变形对郟庐断裂带同造山运动的制约. *地质科学*, 41(1): 102–121
- 朱光, 徐佑德, 刘国生, 王勇生, 谢成龙. 2006b. 郟庐断裂带中-南段走滑构造特征与变形规律. *地质科学*, 41(2): 226–241
- 朱光, 张力, 谢成龙, 牛漫兰, 王勇生. 2009. 郟庐断裂带构造演化的同位素年代学制约. *地质科学*, 44(4): 1327–1342